

## Adaptive NN impedance control for an SEA-driven robot

Xinbo YU<sup>1,2,3</sup>, Wei HE<sup>1,2,3\*</sup>, Yanan LI<sup>4</sup>, Chengqian XUE<sup>1,2,3</sup>,  
Yongkun SUN<sup>1,2,3</sup> & Yu WANG<sup>5</sup>

<sup>1</sup>*School of Automation and Electrical Engineering, University of Science and Technology Beijing, Beijing 100083, China;*

<sup>2</sup>*Institute of Artificial Intelligence, University of Science and Technology Beijing, Beijing 100083, China;*

<sup>3</sup>*Key Laboratory of Knowledge Automation for Industrial Processes, Ministry of Education, University of Science and Technology Beijing, Beijing 100083, China;*

<sup>4</sup>*Department of Engineering and Design, University of Sussex, Brighton BN1 9RH, UK;*

<sup>5</sup>*Institute of Automation, Chinese Academy of Sciences, Beijing 100190, China*

Received 13 September 2018/Accepted 23 October 2018/Published online 25 February 2020

**Citation** Yu X B, He W, Li Y N, et al. Adaptive NN impedance control for an SEA-driven robot. *Sci China Inf Sci*, 2020, 63(5): 159207, <https://doi.org/10.1007/s11432-018-9631-7>

Dear editor,  
Series elastic actuators (SEAs) have been deliberately selected in collaborative robots intended for safe physical interaction with humans or unstructured environments [1]. This passive mechanical compliance guarantees an inertial decoupling between the link and actuator, thus decreasing kinetic energy involved in unexpected collisions with environments [2]. SEAs are widely used in cooperative industrial robots (Baxter robot), humanoid robots (Valkyrie) and rehabilitation robots. Although SEA can avoid damages of collisions with humans or environments, only passive impedance cannot achieve desired impedance due to the fixed mechanical stiffness of SEA [3]. Therefore, it is necessary to combine active impedance control algorithm with passive mechanical compliance. For achieving the accuracy of tracking the desired model, SEA-driven robot's dynamics can be described using a flexible joint model. Considering there exist uncertainties of compliant robot's dynamics, various methods, i.e., iterative learning control [4], adaptive control [5, 6], uncertainty and disturbance estimator (UDE) [7], are used to address this issue and improve the tracking accuracy. In this study, we propose an adaptive active impedance control combined with passive mechanical impedance, and use neural networks (NNs) to

compensate for uncertainties of compliant robot's dynamics. Taking these into account, we propose an online adaptive law to update NN weights and a complete framework about adaptive impedance control design. Simulations show the proposed method can ensure that both the accuracy and safety can be achieved. The contributions of this study are summarized as follows: auxiliary variables are designed for Lyapunov stability analysis and control design; and radial basis function neural networks (RBFNNs) are utilized to compensate for uncertainties in dynamics to improve the accuracy when tracking a desired impedance model.

*N-link SEA-driven robot's dynamic model.* In dynamics described in (1),  $q \in \mathbb{R}^n$ ,  $\vartheta \in \mathbb{R}^n$  denote the joint and motor angle, respectively.  $M_c \in \mathbb{R}^{n \times n}$ ,  $C_c \in \mathbb{R}^{n \times n}$  and  $G_c \in \mathbb{R}^n$  denote the inertia, Coriolis and centrifugal and gravity matrices of robots.  $M_p \in \mathbb{R}^{n \times n}$  and  $K_p \in \mathbb{R}^{n \times n}$  denote motor inertia and mechanical stiffness of SEA.  $\tau \in \mathbb{R}^n$  denotes the input torque and  $\tau_f \in \mathbb{R}^n$  denotes the external torque generated by humans or environments.

$$\begin{aligned} M_c \ddot{q} + C_c \dot{q} + G_c &= K_p(\vartheta - q) - \tau_f, \\ M_p \ddot{\vartheta} + K_p(\vartheta - q) &= \tau. \end{aligned} \quad (1)$$

*Control design.* In this study, the control design is to achieve the following impedance relationship

\* Corresponding author (email: weihe@ieee.org)

for SEA-driven robot:

$$M_d(\ddot{q} - \ddot{q}_d) + D_d(\dot{q} - \dot{q}_d) + K_d(q - q_d) = \tau_f, \quad (2)$$

where  $M_d$ ,  $D_d$  and  $K_d$  denote the desired inertia, damping and stiffness matrices and  $q_d$  denotes the desired angle.

Step 1. Define auxiliary variables  $z$  and  $\eta$ . We define variable  $\varpi$  as  $M_d\ddot{e} + D_d\dot{e} + K_d e - \tau_f$  where  $e = q - q_d$ . We can see that if  $\varpi$  is converging to zero, the target impedance model will be achieved. To facilitate analysis, we define another impedance error  $\omega$  as  $\omega = L_f \varpi = \ddot{e} + L_d \dot{e} + L_k e - L_f \tau_f$ , where  $L_f = M_d^{-1}$ ,  $L_d = M_d^{-1} D_d$ ,  $L_k = M_d^{-1} K_d$ . We choose two positive matrices  $T$  and  $M$  as  $T + M = L_d$ ,  $\dot{T} + TM = L_k$  and  $\dot{\tau}_{rl} + M\tau_{rl} = L_f \tau_f$ . According to these, we rewrite  $\omega$  as

$$\omega = \ddot{e} + (T + M)\dot{e} + (\dot{T} + TM)e - \dot{\tau}_{rl} - M\tau_{rl}. \quad (3)$$

And we define an auxiliary variable  $z$  and rewrite (3) as

$$z = \dot{e} + Te - \tau_{rl}, \quad \omega = \dot{z} + Mz. \quad (4)$$

When  $z$  converges to zero, we can conclude that  $\dot{z} \rightarrow 0$  if its limit exists. We define an virtual state variable matrix  $q_r$  as

$$\dot{q}_r = \dot{q}_d - Te + \tau_{rl}, \quad (5)$$

so  $z$  can be rewritten as

$$z = \dot{q} - \dot{q}_r. \quad (6)$$

Therefore, if  $z \rightarrow 0$ , then  $\varpi \rightarrow 0$ . According to above analysis, we also define an auxiliary variable  $\eta$  about motor angle  $\vartheta$  as

$$\eta = \dot{\vartheta} - \dot{\vartheta}_r = \dot{\vartheta} - \dot{\vartheta}_d + \beta_\vartheta \tilde{\vartheta}, \quad (7)$$

where  $\tilde{\vartheta} = \vartheta - \vartheta_d$ ,  $\beta_\vartheta$  is the positive definite matrix,  $\vartheta_d$  denotes the desired motor angle, and  $\dot{\vartheta}_r = \dot{\vartheta}_d - \beta_\vartheta \tilde{\vartheta}$ .

Step 2. Construct Lyapunov function candidates by using auxiliary variables  $z$  and  $\eta$ . According to (6) and (7), we construct Lyapunov function candidates as follows:

$$V_1 = \frac{1}{2} z^T M_c z + \frac{1}{2} \eta^T M_p \eta + \frac{1}{2} \int_0^t (z - \eta)^T dt K_p \int_0^t (z - \eta) dt. \quad (8)$$

Step 3. Controller design by using backstepping method. Differentiating (8) with respect to time, we have

$$\dot{V}_1 = z^T M_c \dot{z} + \frac{1}{2} z^T \dot{M}_c z + \eta^T M_p \dot{\eta}$$

$$+ (z - \eta)^T K_p \int_0^t (z - \eta) dt = z^T \left( M_c \dot{z} + C_c z + K_p \int_0^t (z - \eta) dt \right) + \eta^T \left( M_p \dot{\eta} - K_p \int_0^t (z - \eta) dt \right). \quad (9)$$

We divide (9) to two parts, and the first part can be calculated as

$$M_c \dot{z} + C_c z + K_p \int_0^t (z - \eta) dt = \zeta_1 + K_p \vartheta_d. \quad (10)$$

Then we define  $K_p \vartheta_d$  as

$$K_p \vartheta_d = -K_1 z - \zeta_1, \quad (11)$$

where  $K_1$  is the gain matrix, then we can get

$$\begin{aligned} \dot{V}_1 &= -z^T K_1 z + \eta^T \left( M_p \dot{\eta} - K_p \int_0^t (z - \eta) dt \right) \\ &= -z^T K_1 z + \eta^T \zeta_2. \end{aligned} \quad (12)$$

where we define

$$\zeta_2 = \tau + \zeta_3. \quad (13)$$

$\zeta_1$ ,  $\zeta_2$  and  $\zeta_3$  are defined as auxiliary variables. We design the following controller:

$$\begin{aligned} \tau &= -K_2 \eta + M_p (\ddot{\vartheta}_d - \beta_\vartheta \dot{\tilde{\vartheta}}) - z + \tau_f + G_c \\ &\quad + M_c (\ddot{q}_d - T\dot{e} + \dot{\tau}_{rl}) + C_c (\dot{q}_d - Te + \tau_{rl}), \end{aligned} \quad (14)$$

where  $K_2$  denotes the gain matrix, and  $\vartheta_d$  is defined as

$$\begin{aligned} \vartheta_d &= K_p^{-1} (-K_1 z + \tau_f + G_c - M_c (-\ddot{q}_d + T\dot{e} - \dot{\tau}_{rl})) \\ &\quad - K_p \left( -q_d - e(0) + \tilde{\vartheta}(0) + \beta_\vartheta \int_0^t (e - \tilde{\vartheta}) dt \right) \\ &\quad - C_c (-\dot{q}_d + Te - \tau_{rl}). \end{aligned} \quad (15)$$

We can see that under the controller (14) and define  $\vartheta_d$  as (15), all error signals are bounded,  $z$  and  $\eta$  converge to zero and  $\ddot{\vartheta}_d$  can be computed from (15). The stability analysis is shown in Appendix A.

Step 4. Adaptive neural networks (NNs) to approximate uncertainties. Seen from (14) and (15), there exist uncertainties about robot's dynamics, i.e.,  $M_c$ ,  $C_c$  and  $G_c$  are unknown. To solve this problem, adaptive NN is employed to approximate uncertainties in dynamics as follows:

$$\begin{aligned} \chi_M^{*T} \phi_M(Z) &= M_c + \epsilon_M, \\ \chi_C^{*T} \phi_C(Z) &= C_c + \epsilon_C, \\ \chi_G^{*T} \phi_G(Z) &= G_c + \epsilon_G, \end{aligned} \quad (16)$$

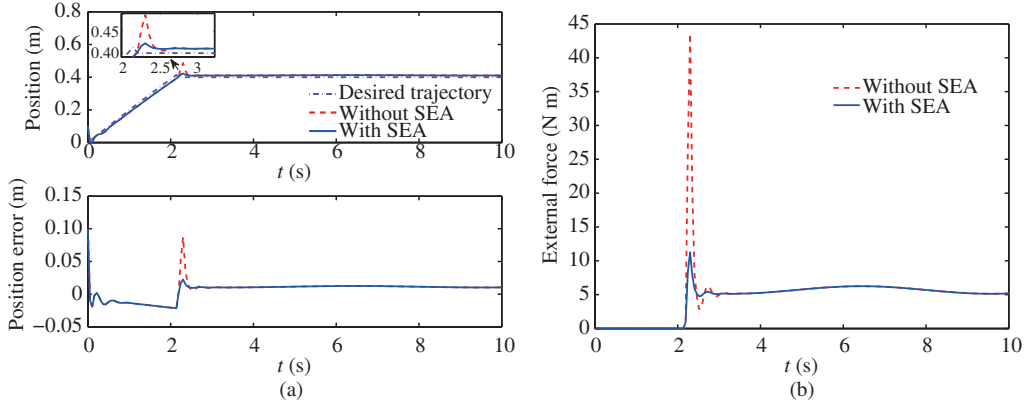


**Figure 1** (Color online) The simulation results. (a) Position and position error; (b) external torque.

where  $\chi_M^*$ ,  $\chi_C^*$  and  $\chi_G^*$  are actual weights,  $\epsilon_M$ ,  $\epsilon_C$  and  $\epsilon_G$  are approximation errors,  $\phi_M(Z)$ ,  $\phi_C(Z)$  and  $\phi_G(Z)$  are basis functions,  $Z$  denotes the input of NN.  $\hat{\chi}_M$ ,  $\hat{\chi}_C$  and  $\hat{\chi}_G$  are estimates of NN weights.  $\tilde{\chi}_M$ ,  $\tilde{\chi}_C$  and  $\tilde{\chi}_G$  are estimation errors which have the relationship  $(\cdot)^* = \hat{(\cdot)} - \tilde{(\cdot)}$ . The adaptation laws are designed as follows:

$$\begin{aligned}\dot{\hat{\chi}}_M &= -\Gamma_M(\phi_M(Z)\dot{A}\eta + \sigma_M\hat{\chi}_M), \\ \dot{\hat{\chi}}_C &= -\Gamma_C(\phi_C(Z)A\eta + \sigma_C\hat{\chi}_C), \\ \dot{\hat{\chi}}_G &= -\Gamma_G(\phi_G(Z) + \sigma_G\hat{\chi}_G),\end{aligned}\quad (17)$$

where  $\Gamma_M$ ,  $\Gamma_C$  and  $\Gamma_G$  denote the positive definite constant gain matrices,  $\sigma_M$ ,  $\sigma_C$  and  $\sigma_G$  denote small positive constants.  $A = \dot{q}_d - Te + \tau_{rl}$ , so we can rewrite (14) and (15) as follows:

$$\begin{aligned}\tau &= -K_2\eta + M_p(\ddot{\vartheta}_d - \beta_\vartheta\dot{\vartheta}) - z + \tau_f + \hat{\chi}_G^T\phi_G(Z) \\ &\quad + \hat{\chi}_M^T\phi_M(Z)\dot{A} + \hat{\chi}_C^T\phi_C(Z)A - K_q\text{sgn}(\eta),\end{aligned}\quad (18)$$

$$\begin{aligned}\vartheta_d &= K_p^{-1}\left(-K_1z + \tau_f + G_c + \hat{\chi}_M^T\phi_M(Z)\dot{A}\right. \\ &\quad \left.+ \hat{\chi}_C^T\phi_C(Z)A - K_p\left(-q_d - e(0) + \tilde{\vartheta}(0)\right.\right. \\ &\quad \left.\left.+ \beta_\vartheta\int_0^t(e - \tilde{\vartheta})dt\right)\right),\end{aligned}\quad (19)$$

where positive gain matrix  $K_q \geq \|\epsilon_M\dot{A} + \epsilon_C A + \epsilon_G\|$ ,  $\text{sgn}(\cdot)$  returns a vector with the signs of the corresponding elements of the vector  $(\cdot)$ . Under the RBFNN controller (18) and by defining (19), we can achieve the control objective (2). And we choose a Lyapunov candidates  $V_2$  as follows:

$$\begin{aligned}V_2 &= \frac{1}{2}z^T M_c z + \frac{1}{2}\eta^T M_p \eta \\ &\quad + \frac{1}{2}\int_0^t (z - \eta)^T dt K_p \int_0^t (z - \eta) dt + \frac{1}{2}\tilde{\chi}_M^T \Gamma_M^{-1} \tilde{\chi}_M \\ &\quad + \frac{1}{2}\tilde{\chi}_C^T \Gamma_C^{-1} \tilde{\chi}_C + \frac{1}{2}\tilde{\chi}_G^T \Gamma_G^{-1} \tilde{\chi}_G.\end{aligned}\quad (20)$$

The stability analysis is shown in Appendix B.

Step 5. Simulation results. The simulation results are shown in Figure 1, and we can see that the external force with SEA is smaller than the external force without SEA when physical collisions occur. The simulation settings and processes are described in Appendix C.

**Acknowledgements** This work was supported by National Natural Science Foundation of China (Grant No. 61873298), China Postdoctoral Science Foundation (Grant No. 2018M630074), and Beijing Science and Technology Project (Grant No. Z181100003118006).

**Supporting information** Appendixes A–C. The supporting information is available online at [info.scichina.com](http://info.scichina.com) and [link.springer.com](http://link.springer.com). The supporting materials are published as submitted, without typesetting or editing. The responsibility for scientific accuracy and content remains entirely with the authors.

## References

- He W, Li Z, Chen C L P. A survey of human-centered intelligent robots: issues and challenges. *IEEE/CAA J Autom Sin*, 2017, 4: 602–609
- Li Z, Huang B, Ajoudani A, et al. Asymmetric bimanual coordinate control of dual-arm exoskeleton robots for human cooperative manipulations. *IEEE Trans Robot*, 2018, 34: 264–271
- Vallery H, Veneman J, van Asseldonk E, et al. Compliant actuation of rehabilitation robots. *IEEE Robot Automat Mag*, 2008, 15: 60–69
- Li Y, Ge S S. Impedance learning for robots interacting with unknown environments. *IEEE Trans Contr Syst Technol*, 2014, 22: 1422–1432
- Chen M. Disturbance attenuation tracking control for wheeled mobile robots with skidding and slipping. *IEEE Trans Ind Electron*, 2017, 64: 3359–3368
- Yang C, Wang X, Cheng L, et al. Neural-learning-based telerobot control with guaranteed performance. *IEEE Trans Cybern*, 2017, 47: 3148–3159
- Dong Y T, Ren B B. UDE-based variable impedance control of uncertain robot systems. *IEEE Trans Syst Man Cybern Syst*, 2017. doi: 10.1109/TSMC.2017.2767566